Journal of Electronic Materials (2022) 51:7164–7172
https://doi.org/10.1007/s11664-022-09955-3

ORIGINAL RESEARCH ARTICLE

Fabrication and Electrical Characterization of Ti/p-Si Metal Semiconductor Schottky Structures at Low Temperature

H. Asil Uğurlu[1]

Received: 1 June 2022 / Accepted: 12 September 2022 / Published online: 30 September 2022
© The Minerals, Metals & Materials Society 2022

Abstract

Temperature-dependent electrical analysis of the Ti/p-Si/Al Schottky barrier diode was performed by measuring the current–voltage (*I*–*V*) and capacitance–voltage (*C*–*V*) properties over a temperature range of 80–300 K in steps of 20 K. Electrical parameters including the barrier height (Φ_{b0}) and ideality factor (n) were calculated according to the thermionic emission (TE) theory. It was determined that the barrier height values increased and the values of the ideality factor decreased with the increase in temperature. The temperature-dependent barrier height properties were explained by considering the barrier height inhomogeneity using a Gaussian distribution. From the $1/2kT$ versus Φ_{b0} graph, which shows the Gaussian distribution, the mean barrier heights and standard deviation were 0.5856 eV and 67 mV (80–160 K) and 1.0443 eV and 129 mV (180–300 K), respectively. The temperature dependence of the Ti/p-Si Schottky barrier diode (SBD) is explained based on the TE mechanism and Gaussian distribution of the barrier heights. In addition, the barrier heights determined from the *C*–*V* measurements are higher than the values obtained from the *I*–*V* measurements in conjunction with the formation of an inhomogeneous Schottky barrier at the interface.

Keywords Ti/p-Si SBDs · temperature dependence · Gaussian distribution · barrier inhomogeneity

Introduction

Metal–semiconductor (MS) contacts are basic devices widely used in modern technology, particularly in the electronics industry. Schottky barrier diodes (SBDs), comprising M–S interfaces, are the basis of many electronic devices, photodetectors, field-effect transistors, solar cells, and microwave diodes. Due to the technological importance of SBDs, a thorough understanding of their electrical behavior is critical. It is well known that metal–semiconductor interface states have a dominant effect on device performance, stability, and reliability.[1–4]

Furthermore, studies conducted only at room temperature or in a small temperature range do not provide detailed information about barrier formation or current conduction mechanisms at the M–S interface.[5–7] On the other hand, knowing the temperature dependence of the current–voltage (*I*–*V*) properties for a wide temperature range allows us to understand different directions of the underlying device properties and conduction mechanisms.[8,9] The thermionic emission (TE) theory is normally used to determine diode parameters such as zero-bias barrier height (Φ_b), and according to TE theory, the ideality factor (n) is expected to be close to unity. However, the obtained value of the ideality factor is usually greater than 1, especially at low temperatures, which can be attributed to the presence of an insulating layer at the M–S interface, the spatial distribution of the interfacial states in the semiconductor band gap, or the reduction of the image force of the barrier.[10–13]

Additionally, experimental analysis of the *I*–*V* properties based on the TE mechanism often shows an abnormal decrease in Φ_b and an increase in n with decreasing temperature, resulting in nonlinear behavior of $1/T$ versus $\ln(I_0/T^2)$ in activation energy graphs.[12,14–16] In recent studies, the temperature dependence of n and Φ_b, and the nonlinear behavior of the activation graphs at low temperatures have been successfully explained by considering the Gaussian distribution and TE mechanism.[10,15,17,18] Spatial barrier inhomogeneities in SBDs are mainly defined by the Gaussian distribution

✉ H. Asil Uğurlu
haticeasil@isparta.edu.tr

[1] Department of Mechatronics, Isparta OSB Vocational School, Isparta University of Applied Sciences, 32200 Isparta, Turkey

function, which has been widely used for correlating experimental data.[10–18]

Various elements, including aluminum (Al),[1,19] tin (Sn),[12,20] titanium (Ti),[21,22] nickel (Ni),[23] lead (Pb),[4] and silver (Ag),[24,25] have been used to produce Schottky contacts on p-Si. For example, Aboelfotoh[21] formed the Ti/Si structure for both n-Si and p-Si semiconductors and examined the changes in the barrier height and ideality factor by investigating the effects of annealing and temperature. Having examined the *I–V* characteristics using 40 K intervals between 95 K and 295 K for p-Si, he found ideality factor values between 1.22 (95 K) and 1.13 (295 K) and a barrier height of 0.623 eV (295 K). Aydın et al.[20] investigated Sn/p-Si in the temperature range of 80–300 K, and the Φ_b and Richardson's constant A^* obtained from the modified $\ln(I_0/T^2) - (q^2\sigma^2/k^2T^2)$ versus 1/kT graph were 0.95 eV and 15.6 $Acm^{-2}\ K^{-2}$, respectively. Similarly, Karataş et al.[12] calculated the Φ_b and Richardson constant A^* values as 1.026 eV and 14.60 $Acm^{-2}\ K^{-2}$ using measurements of the Sn/p-Si diode in the temperature range of 150–400 K.

In this study, the *I–V* and capacitance–voltage (*C–V*) properties of Ti SBDs fabricated on a p-Si semiconductor were investigated in the temperature range of 80–300 K. The temperature-dependent properties of Ti/p-Si SBDs were examined based on a Gaussian distribution of the barrier height around a mean value due to the presence of barrier inhomogeneities at the M–S interface.

Experimental Methods

The Ti/p-Si Schottky diodes were fabricated using previously cleaned p-type Si wafers with (100) orientation and 5–10 Ωcm resistivity. The wafers were chemically rinsed using the general RCA cleaning procedure (10 min boiling in $NH_4 + H_2O_2 + 6H_2O$ followed by 10 min boiling in $HCl + H_2O_2 + 6H_2O$). The native oxide on the front surface of p-Si was removed in $HF:H_2O$ (1:10) solution, and finally the wafer was rinsed in deionized (DI) water for 30 s. Then, a low-resistivity ohmic back contact was made using Al, followed by temperature treatment at 570°C for 3 min in N_2 atmosphere. The Schottky contacts were formed by evaporation of Ti dots with diameters of about 1.0 mm (diode area $= 7.85 \times 10^{-3}$ cm^2). All evaporation processes were carried out in a vacuum coating chamber at about 1.3332×10^{-6} kPa. The *I–V* and *C–V* characteristics were measured using a temperature-controlled Leybold-Heraeus closed-loop helium cryostat over a temperature range of 80–300 K in steps of 20 K in the dark. The *I–V* measurements of this structure were performed with a Keithley 487 picoammeter/voltage source, and the *C–V* measurements were performed at 500 kHz with an HP 4192A LF impedance analyzer.

Results and Discussion

For a nonideal SBD, passage of current is mostly achieved by mobile charge carriers and described by TE theory. According to TE theory, the passage of current through the M–S junction is expressed in Eq. 1.[2]

$$I = I_0 \exp\left(\frac{qV}{nkT}\right)\left[1 - exp\left(-\frac{qV}{kT}\right)\right] \tag{1}$$

Here, k is the Boltzmann constant, q is the electric charge, V is the voltage applied across the junction, T is the temperature in Kelvin, and n is the ideality factor. I_0 is the saturation current obtained from the straight-line intersection of ln I at V = 0. I_0 is calculated using Eq. 2.

$$I_0 = AA^*T^2 \exp\left(-\frac{q\Phi_{b0}}{kT}\right) \tag{2}$$

Here, A is the effective area of the diode, A^* is the Richardson constant, which has a value for p-Si of 32 $Acm^{-2}\ K^{-2}$,[3,26] and Φ_{b0} is the barrier height at zero bias. The calculated I_0 value is used to determine the Φ_{b0} of SBDs, and Φ_{b0} is obtained by rewriting Eq. 2 as expressed below.

$$\Phi_{b0} = \frac{kT}{q} In\left(\frac{AA^*T^2}{I_0}\right) \tag{3}$$

The ideality factor n is calculated from the slope of the forward bias *I–V* graphs, as expressed below.

$$n = \frac{q}{kT}\left(\frac{dV}{d(lnI)}\right) \tag{4}$$

The Φ_{b0} and n of SBDs are calculated as a function of temperature using Eqs. 3 and 4.

The forward and reverse bias *C–V* characteristics of the Ti/p-Si SBD in the temperature range of 80–300 K using 20 K steps are shown in Fig. 1. The calculated I_0 of the SBDs ranges from 4.49×10^{-13} A (at 80 K) to 8.89×10^{-9} A (at 300 K) at a voltage of 0.0 V. As seen in Fig. 1, the forward current increases exponentially with applied voltage and temperature. Therefore, the behavior of the *C–V* curves shows a strong dependence on temperature. *C–V* curves at several temperatures contain more information for understanding the important electrical parameters of the Ti/p-Si SBD. Using Eqs. 3 and 4, the Φ_{b0} and n were calculated and plotted as a function of temperature (Fig. 2). As shown in Fig. 2 and Table I, Φ_{b0} increased and n decreased with increasing temperature ($n = 3.77$ and $\Phi_{b0} = 0.267$ eV at 80 K, $n = 1.43$ and $\Phi_{b0} = 0.738$ eV at 300 K). In other words, both parameters were strongly dependent on the temperature. Since current transfer across the M–S interface depends on temperature, the current flow at low temperatures is generated by the carriers

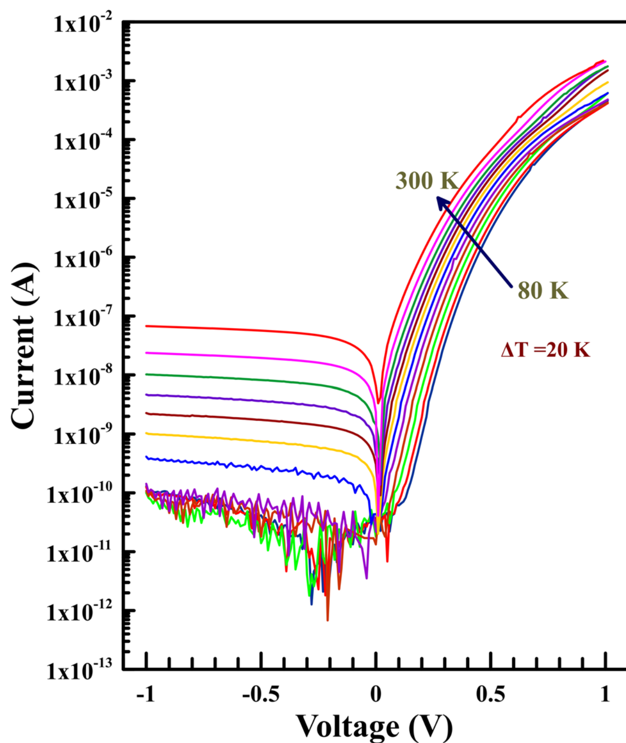

Fig. 1 The *C–V* characteristics of the Ti/p-Si SBD as a function of temperature.

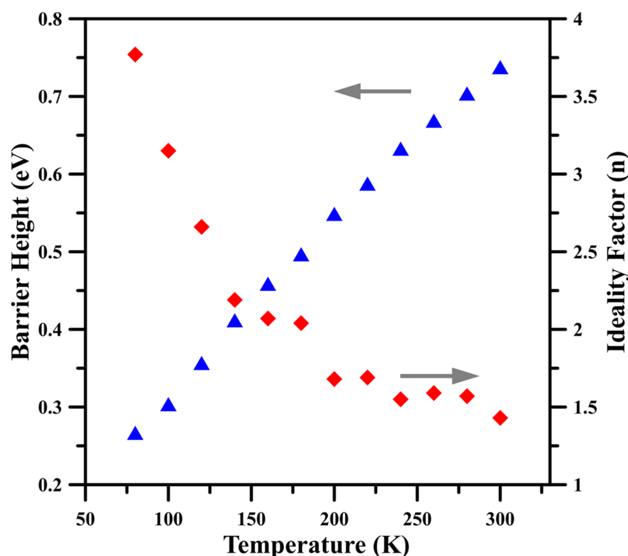

Fig. 2 The ideality factor and barrier height variation in the temperature range of 80–300 K for the Ti/p-Si SBD.

with energy that exceeds lower barriers. Accordingly, the barrier height decreases as the ideality factor increases at lower temperatures. Still, as more charge carriers gain sufficient thermal energy to exceed the barrier at high temperatures, more electrons will have the energy to exceed

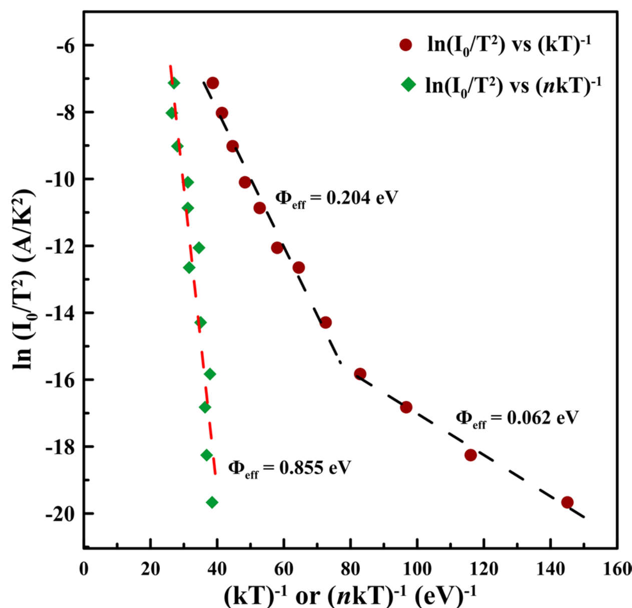

Fig. 3 Conventional activation curves of the $\ln(I_0/T^2)$ versus $(kT)^{-1}$ and $(nkT)^{-1}$ for the Ti/p-Si SBD.

the higher barrier, and the barrier height also increases with temperature and forward bias voltage.[4,7,8,11,13]

Richardson graphs of I_0 can alternatively be used to calculate the Φ_{b0} (Fig. 3). To plot this graph, the natural logarithmic of Eq. 2 is taken and rewritten as expressed below.

$$ln\left(\frac{I_0}{T^2}\right) = \ln(AA^*) - \frac{q\Phi_{b0}}{nkT} \tag{5}$$

According to Eq. 5, the $\ln(I_0/T^2)$ versus $1/kT$ graph is expected to yield a straight line, and the point where the graph intersects the axis gives the A^* values. Furthermore, the slope of this graph gives the barrier height at $T=0$ K, and this value is also called the activation energy (Φ_{eff}). Activation energy can be defined as the energy barrier that must be overcome for a chemical reaction to occur, or the minimum energy required to initiate a chemical reaction. At high temperatures, the activation energy is equal to the energy to create holes, which is the sum of the energy required for generating holes and the movement of charge carriers to those metastable positions.[27]

As shown in Fig. 3, the temperature dependence of $\ln(I_0/T^2)$ versus $1/kT$ was linear in the two temperature ranges, 80–140 K and 160–300 K. By curve fitting the experimental data, the Φ_{eff} was 0.204 eV at high temperatures (160–300 K) and 0.062 eV at lower temperatures (80–140 K). The A^* values were calculated as 1.60×10^2 Acm^{-2} K^{-2} (160–300 K) and 2.53×10^{-3} Acm^{-2} K^{-2} (80–140 K) for Ti/p-Si. Similarly, the graph of $\ln(I_0/T^2)$ versus $1/nkT$ exhibited a linear behavior in the temperature

range of 80–300 K, and the Φ_{eff} was 0.855 eV and A^* was 6.39×10^8 $\mathrm{Acm^{-2}\,K^{-2}}$.

The deviations in Richardson graphs may be due to spatially inhomogeneous barrier heights, potential fluctuations at the interface containing low and high barrier regions, and differences between the real and calculated effective masses.[8,24,28]

An abnormal behavior observed during temperature-dependent I–V measurements of SBDs is normally attributed to the inhomogeneity of the barrier height. This inhomogeneity can be described by the Gaussian distribution, which includes the mean barrier height ($\overline{\Phi}_{b0}$) and the standard deviation (σ_0), which represents the homogeneity of the M–S interface.[10,17,24,29,30] Expressions for apparent barrier height (Φ_{ap}) and apparent ideality factor (n_{ap}) are given below.

$$\Phi_{ap} = \overline{\Phi}_{b0} - \frac{q\sigma_0^2}{2kT} \quad (6)$$

$$\frac{1}{n_{ap}} - 1 = -\rho_2 + \frac{q\rho_3}{2kT} \quad (7)$$

Here, ρ_2 and ρ_3 are the voltage coefficients that can be temperature dependent and determine the amount of voltage deformation of the barrier height distribution. However, the mean value of the standard deviation and the Schottky barrier height are assumed to be linearly related to the Gaussian parameters. The mean value of the Schottky barrier height and standard deviation are generally written as $\overline{\Phi}_b = \overline{\Phi}_{b0} + \rho_2 V$ and $\sigma_s = \sigma_0 + \rho_3 V$, where ρ_2 is the temperature-dependent voltage coefficient and ρ_3 is the coefficient determining the amount of voltage deformation on the barrier height.[31,32] Figure 4 shows the experimental Φ_{ap} versus $1/2kT$ graph. The standard deviation of the distribution and the mean barrier height values were calculated from the point where the graph intersects the axis and the slope with the help of Eq. 6, respectively. Two different distributions were observed for Φ_{ap} and σ_0 values, in the temperature ranges of 80–160 K and 180–300 K. The Φ_{ap} and σ_0 values were determined as 0.5856 eV and 67 mV (Distribution 2) in the temperature range of 80–160 K, and 1.0443 eV and 129 mV (Distribution 1) in the temperature range of 180–300 K. The $(1/n-1)$ versus $1/2kT$ graph should be a straight line giving the voltage coefficients ρ_2 and ρ_3 from the intersection and slope, respectively. According to the graph given in Fig. 5, $\rho_2 = 0.1878$ and $\rho_3 = -0.0083$ V. If the Richardson graph is rewritten by combining Eqs. 2 and 6, then we get the expression below.

$$ln\left(\frac{I_0}{T^2}\right) - \left(\frac{q^2\sigma_0^2}{2k^2T^2}\right) = \ln(AA^*) - \frac{q\overline{\Phi}_{b0}}{kT} \quad (8)$$

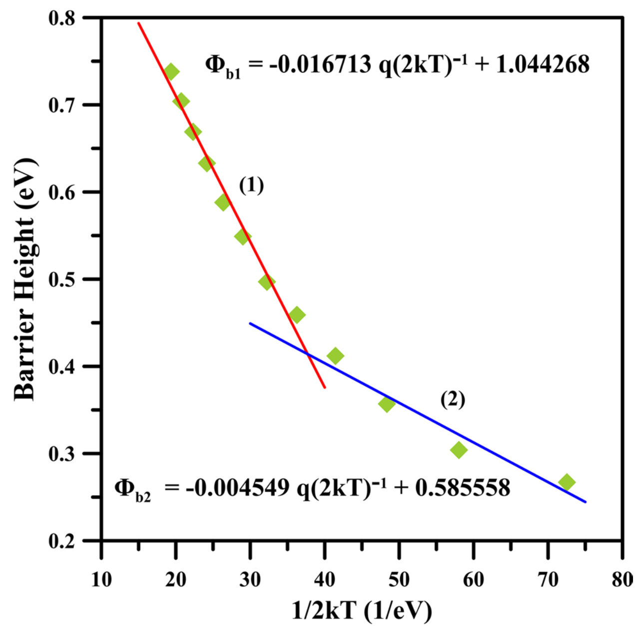

Fig. 4 The zero bias apparent barrier height (Φ_{ap}) versus (1/2kT) plot for the Ti/p-Si SBD.

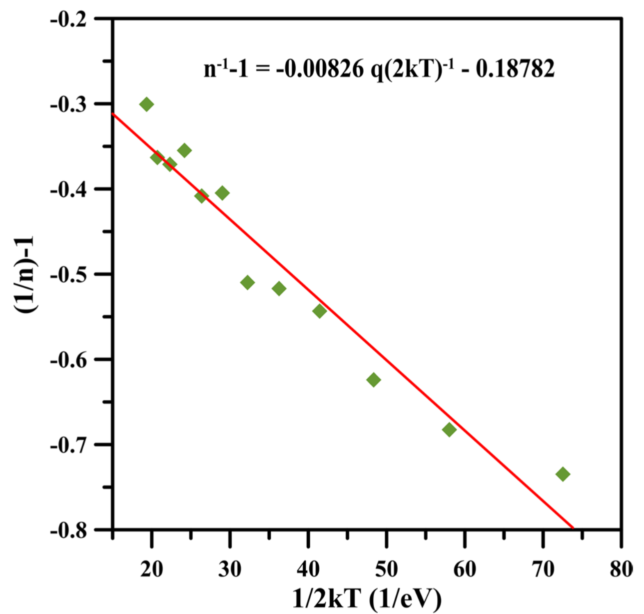

Fig. 5 The ideality factor versus (1/2kT) plot for the Ti/p-Si SBD.

The point where the graph of modified $\ln(I_0/T^2) - (q^2\sigma^2/k^2T^2)$ versus $1/kT$, according to Eq. 8, intersects the axis (ln AA^*) is the Richardson constant A^* and its slope represents the average $\overline{\Phi}_{b0}$. The values of the term $\ln(I_0/T^2) - (q^2\sigma^2/k^2T^2)$ were calculated for the two σ_o

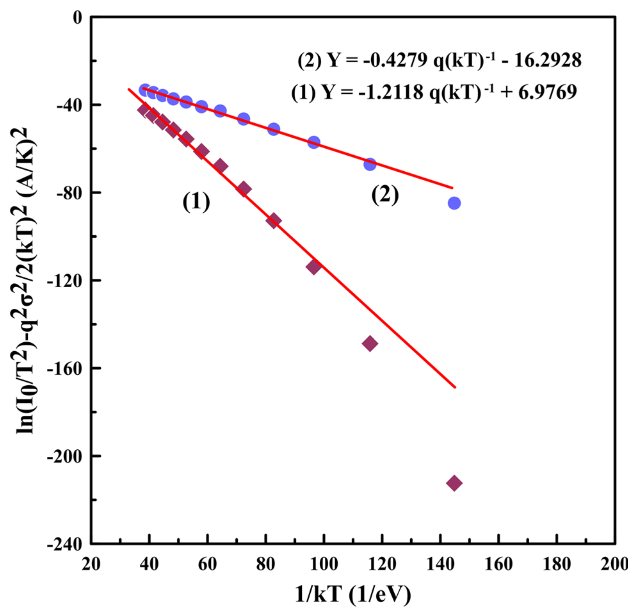

Fig. 6 Modified activation energy ($\ln(I_0/T^2) - q^2\sigma^2/2k^2T^2$ versus 1/ kT) plots for the Ti/p-Si SBD according to Gaussian distribution of the barrier height.

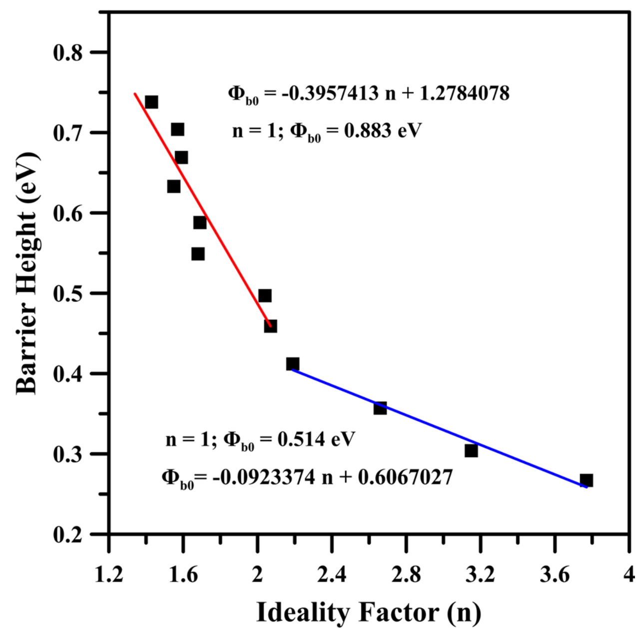

Fig. 7 The zero-bias barrier height versus ideality factor for the Ti/p-Si SBD.

values obtained for the temperature ranges of 80–160 K and 180–300 K. From the graph in Fig. 6, the $\overline{\Phi}_{b0}$ was observed to be 1.2118 eV (180–300 K: (1) Y equation) and 0.4279 eV (80–160 K: (2) Y equation), which are close to the values of $\overline{\Phi}_{b0}$ obtained from the Φ_{ap} versus 1/2kT graph in Fig. 4. Likewise, A^* values were 136,503.1 $\text{Acm}^{-2}\ \text{K}^{-2}$ in the 180–300 K range and 1.069×10^{-5} $\text{Acm}^{-2}\ \text{K}^{-2}$ in the 80–160 K range.

Tung's theoretical approach[11,33] suggests that there is a linear relationship between ideality factors and experimental zero-bias barrier heights, i.e., n and Φ_{b0}. The graph of Φ_{b0} versus n for the Ti/p-Si SBD is given in Fig. 7, which indicates that the two variables are inversely proportional. Between the values of Φ_{b0} and n, there are two linear regions that can be explained by the lateral inhomogeneity of the barrier heights. In region I (160–300 K), the barrier height value from extrapolation to $n = 1$ was 0.883 eV, which is close to the band gap of Si, and in region II (80–140 K), the barrier height was 0.514 eV, approximately half of the Si band gap. This result indicates that, under forward bias, the current flow is controlled by TE for the temperature range $T \geq 160$ K and by thermionic field emission (TFE) for $T \leq 160$ K.[2,3] These findings confirm that the dominant current flow is based on TE and a double Gaussian distribution of the barrier height can be observed in SBDs.[6,34]

Moreover, C–V measurements are widely relied upon to determine the fundamental properties of SBDs such as barrier height, diffusion potential, semiconductor carrier concentration, and Fermi level. The depletion region capacitance on a p-type semiconductor structure for C–V measurements can be expressed as shown in Eq. 9.[24,35]

$$\frac{1}{C^2} = \frac{2(V_d + V)}{\varepsilon_0 \varepsilon_s q A^2 N_A} \tag{9}$$

Here, V_d is the diffusion potential, V is the applied voltage, and N_A is the acceptor concentration of the Si semiconductor. The x-intercept of the graph of C^{-2} versus V represents the diffusion potential. The barrier height calculated from the C–V measurement, $\Phi_{(C-V)}$, at different temperatures is expressed below.

$$\Phi_{(C-V)} = V_i + \frac{kT}{q} + kT\ln\left(\frac{N_V}{N_A}\right) - \Delta\Phi_b = V_d + E_F - \Delta\Phi_b \tag{10}$$

E_F is the potential difference between the valence band edge and the Fermi level in the neutral region of p-type Si, and $\Delta\Phi_b$ is the image force barrier, which is calculated using Eq. 11.

$$\Delta\Phi_b = \sqrt{\frac{qE_m}{4\pi\varepsilon_s\varepsilon_0}} \tag{11}$$

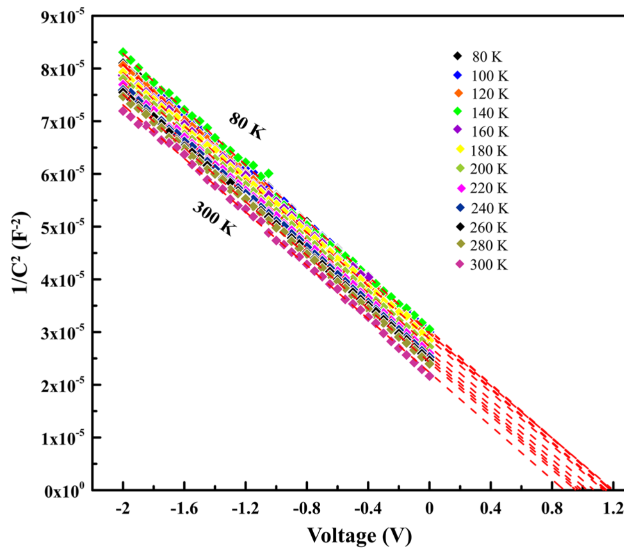

Fig. 8 C^{-2}–V characteristics of the Ti/p-Si SBD in the temperature range of 80–300 K.

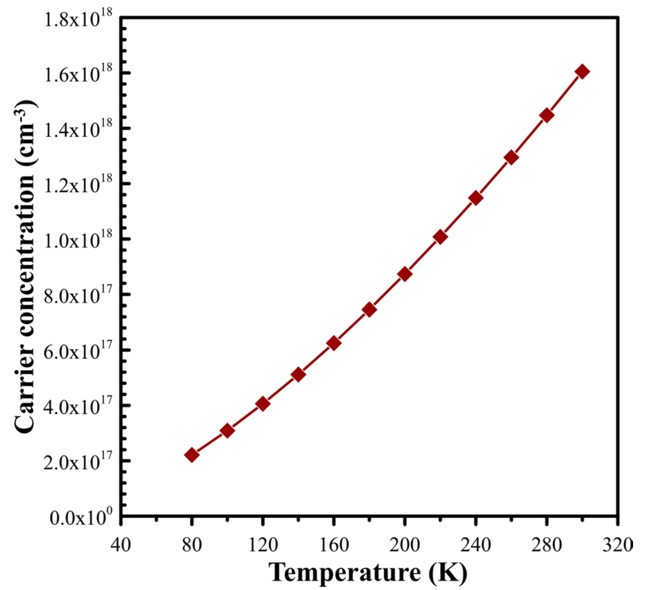

Fig. 9 The variation in carrier density with temperature for the Ti/p-Si SBD.

Here, E_m is the maximum electric field, $E_m = \sqrt{2qN_AV_d/\varepsilon_s\varepsilon_0}$. The C^{-2} versus V graph is shown in Fig. 8. The experimental dopant density values, N_A, used in the calculations were determined from the slope of this graph. The temperature-dependent E_F values are obtained from the following expressions.

$$E_F = \frac{kT}{q}\ln\left(\frac{N_v}{N_A}\right) \tag{12}$$

$$N_V = 4.82 \times 10^{15}T^{3/2}\left(\frac{m_h^*}{m_0}\right)^{3/2} \tag{13}$$

Here, N_V is the effective density of states in the valence band of the Si semiconductor, $m_h^* = 0.16\ m_0$ is the effective mass of the holes,[12] and m_0 is the remaining mass of the electron. As seen in Table II and Fig. 9, the N_V was strongly dependent on temperature. The N_V values ranged from 2.210×10^{17} to 16.048×10^{17} cm^{-3} in the temperature range of 80–300 K, and the carrier density increased with increasing temperature. The acceptor concentration values, N_A, ranged from 77.692×10^{15} cm^{-3} to 7.601×10^{15} cm^{-3} and decreased with decreasing temperature. In addition, the temperature-dependent values of the E_F, V_d, $\Delta\Phi_b$ and $\Phi_{(C-V)}$ are listed in Table II. The graph of $\Phi_{(C-V)}$ versus temperature, obtained from the reverse bias C^{-2}–V curves as a function of temperature and using Eq. 10, is presented in Fig. 10. From the experimental $\Phi_{(C-V)}$ curve, $\Phi_{(C-V)}$(T = 0) was 1.35 eV and the temperature coefficient (α) was −1.03 meV/K. Close examination of Tables I and II shows that the $\Phi_{(C-V)}$ values obtained from the C–V characteristics are higher than the Φ_b values obtained from the I–V characteristics. Differences in Φ_b values calculated from I–V and C–V measurements may be due to the presence of an insulating

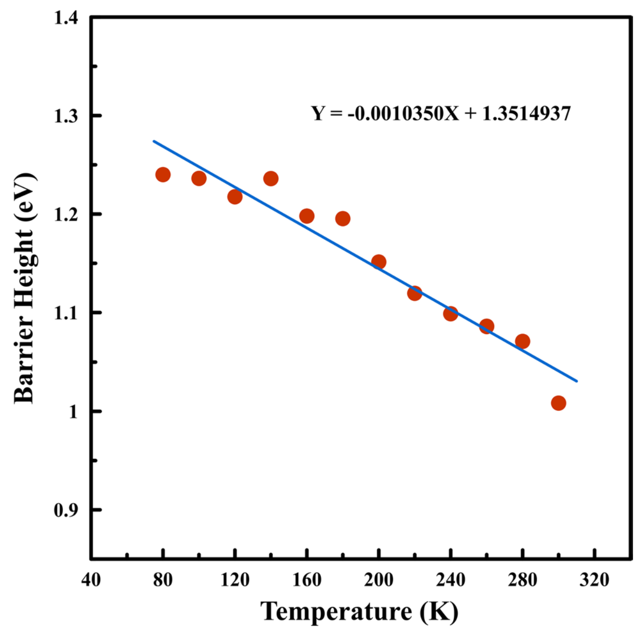

Fig. 10 Temperature dependence of barrier height for the Ti/p-Si SBD obtained from C–V measurements.

layer or charges at the M–S interface, deep contamination levels, leakage currents, and lowering of the image force barrier.[27]

Conclusion

Forward and reverse bias *I–V* and *C–V* properties of Ti/p-Si SBD were measured in the temperature range of 80–300 K. With increasing temperature, the ideality factor values decreased from 3.77 to 1.43, and the values of *I–V* barrier heights increased from 0.267 eV to 0.738 eV. The nature of the temperature-dependent behaviors of ideality factor and barrier height in Ti/p-Si SBDs was explained based on Gaussian distributions of the barrier heights and thermionic emission theory. The results suggest that the presence of deep energy levels near the Ti/Si interface is responsible for creating stored charge and compensates for some of the doping atoms in this region.[36] Gaussian distribution of the barrier height was implemented, and we calculated the mean barrier height values and standard deviation from the graph of Φ_{ap} versus $1/2kT$ as $\overline{\Phi}_{b0} = 0.5856$ eV and $\sigma_0 = 67$ mV (80–160 K) and $\overline{\Phi}_{b0} = 1.0443$ and $\sigma_0 = 129$ mV (180–300 K). According to the modified $\ln(I_0/T^2) - (q^2\sigma^2/k^2T^2)$ versus $1/kT$ graph, Richardson constant A^* and mean barrier height values are $A^* = 136{,}503.1$ Acm^{-2} K^{-2}, $\overline{\Phi}_{b0} = 1.2118$ eV (180–300 K) and $A^* = 1.069 \times 10^{-5}$ Acm^{-2} K^{-2}, $\overline{\Phi}_{b0} = 0.4279$ eV (between 80 K and 160 K). The barrier heights (at $n = 1$) obtained from the linear relationship between the barrier height and the ideality factor were found to be 0.514 eV and 0.883 eV for the temperature ranges of 80–140 K and 160–300 K, respectively. Additionally, the $\Phi_{(I-V)}$ values obtained from the forward bias *I–V* plot are smaller than the $\Phi_{(C-V)}$ values determined from the reverse bias *C–V* properties. The inconsistency between *I–V* and *C–V* barrier height values may be due to the presence of an insulating layer or stored charges at the M–S interface, deep contamination levels, leakage currents, or the image force barrier.

Table I Temperature-dependent values of various diode parameters determined from *I–V* characteristics of Ti/p-Si Schottky barrier diodes

T (K)	I_0 (A)	n	Φ_b (eV)	$\ln(I_0/T^2)$ (A/K^2)	$(2kT)^{-1}$ (eV)$^{-1}$
300	8.89×10^{-9}	1.43	0.738	−7.13	19.341
280	4.16×10^{-9}	1.57	0.704	−8.03	20.722
260	1.79×10^{-9}	1.59	0.669	−9.02	22.316
240	7.14×10^{-10}	1.55	0.633	−10.10	24.176
220	3.94×10^{-10}	1.69	0.588	−10.87	26.374
200	1.45×10^{-10}	1.68	0.549	−12.06	29.011
180	9.92×10^{-11}	2.04	0.497	−12.65	32.235
160	2.43×10^{-11}	2.07	0.459	−14.29	36.264
140	6.80×10^{-12}	2.19	0.412	−15.83	41.445
120	3.43×10^{-12}	2.66	0.357	−16.82	48.352
100	1.18×10^{-12}	3.15	0.304	−18.26	58.023
80	4.49×10^{-13}	3.77	0.267	−19.67	72.528

Table II Temperature-dependent values of various electrical parameters determined from *C–V* characteristics of Ti/p-Si SBD

T (K)	Diffusion potential (V)	Fermi energy (eV)	Carrier concentration 10^{17} (cm^{-3})	Acceptor concentration 10^{15} (cm^{-3})	Image force barrier (meV)	Barrier height (eV)
80	1.217	0.023	2.210	7.692	0.808	1.240
100	1.204	0.032	3.089	7.662	0.805	1.236
120	1.176	0.041	4.060	7.661	0.800	1.218
140	1.185	0.051	5.116	7.595	0.800	1.236
160	1.137	0.061	6.251	7.629	0.793	1.198
180	1.124	0.071	7.459	7.641	0.791	1.195
200	1.070	0.082	8.736	7.634	0.781	1.151
220	1.027	0.093	10.078	7.624	0.773	1.119
240	0.995	0.104	11.483	7.611	0.766	1.099
260	0.971	0.115	12.949	7.613	0.762	1.086
280	0.944	0.127	14.471	7.594	0.756	1.071
300	0.870	0.138	16.048	7.601	0.741	1.008

Conflict of interest I declare that there was no conflict of interest during the planning, execution, and writing of the article.

References

1. İ Dökme, The analysis of I–V characteristics of Schottky diodes by thermionic emission with a Gaussian distribution of barrier height. *Microelectron. Reliab.* 51, 360 (2011). https://doi.org/10.1016/j.microrel.2010.08.017.
2. E.H. Rhoderick and R.H. Williams, *Metal-Semiconductor Contacts*, 2nd ed., (Oxford: Clarendon Press, 1988).
3. S.M. Sze, *Physics of Semiconductor Devices*, 2nd ed., (New York: Wiley, 1981).
4. Ç. Nuhoğlu, E. Özerden, and A. Türüt, The dependence of I–V and C–V characteristics on temperature in the H-terminated Pb/p-Si(1 0 0) Schottky barrier diodes. *Appl. Surf. Sci.* 250, 203 (2005). https://doi.org/10.1016/j.apsusc.2004.12.047.
5. F.E. Cimilli, M. Sağlam, H. Efeoğlu, and A. Türüt, Temperature-dependent current–voltage characteristics of the Au/n-InP diodes with inhomogeneous Schottky barrier height. *Physica B* 404, 1558 (2009). https://doi.org/10.1016/j.physb.2009.01.018.
6. I. Jyothi, V. Janardhanam, H. Hong, and C.-J. Choi, Current–voltage and capacitance–voltage characteristics of Al Schottky contacts to strained Si-on-insulator in the wide temperature range. *Mater. Sci. Semicond. Process.* 39, 390 (2015). https://doi.org/10.1016/j.mssp.2015.05.043.
7. Z. Orhan, A. Taşer, B. Güzeldir, and M. Sağlam, The temperature dependence of current-voltage characteristics of CuAuAg/n-Si/Ti Schottky diode. *Mater. Today Proc.* 46, 6924 (2021). https://doi.org/10.1016/j.matpr.2021.01.560.
8. A.K. Bilgili, T. Güzel, and M. Özer, Current–voltage characteristics of Ag/TiO_2/n-InP/Au Schottky barrier diodes. *J. Appl. Phys.* 125, 5704 (2019). https://doi.org/10.1063/1.5064637.
9. H. Çetin and E. Ayyıldız, Temperature dependence of electrical parameters of the Au/n-InP Schottky barrier diodes. *Semicond. Sci. Technol.* 20, 625 (2005). https://doi.org/10.1088/0268-1242/20/6/025.
10. J.H. Werner and H.H. Güttler, Barrier inhomogeneities at Schottky contacts. *J. Appl. Phys.* 69, 1522 (1991). https://doi.org/10.1063/1.347243.
11. R.T. Tung, Electron transport at metal-semiconductor interfaces: General theory. *Phys. Rev. B* 45, 13509 (1992). https://doi.org/10.1103/PhysRevB.45.13509.
12. Ş Karataş, Ş Altındal, A. Türüt, and A. Özmen, Temperature dependence of characteristic parameters of the H-terminated Sn/p-Si(100) Schottky contacts. *Appl. Surf. Sci.* 217, 250 (2003). https://doi.org/10.1016/S0169-4332(03)00564-6.
13. J.P. Sullivan, R.T. Tung, M.R. Pinto, and W.R. Graham, Electron transport of inhomogeneous Schottky barriers: a numerical study. *J. Appl. Phys.* 70, 7403 (1991). https://doi.org/10.1063/1.349737.
14. S. Chand and J. Kumar, Effects of barrier height distribution on the behavior of a Schottky diode. *J. Appl. Phys.* 82, 5005 (1997). https://doi.org/10.1063/1.366370.
15. A. Gümüş, A. Türüt, and N. Yalçın, Temperature dependent barrier characteristics of CrNiCo alloy Schottky contacts on n-type molecular-beam epitaxy GaAs. *J. Appl. Phys.* 91, 245 (2002). https://doi.org/10.1063/1.1424054.
16. V. Janardhanam, K.A. Ashok, R.V. Rajagopal, and R.P. Narasimha, Study of current–voltage–temperature (I–V–T) and capacitance–voltage–temperature (C–V–T) characteristics of molybdenum Schottky contacts on n-InP (100). *J. Alloys Compd.* 485, 467 (2009). https://doi.org/10.1016/j.jallcom.2009.05.141.
17. C. Coşkun, M. Biber, and H. Efeoğlu, Temperature dependence of current–voltage characteristics of Sn/p-GaTe Schottky diodes. *Appl. Surf. Sci.* 211, 360 (2003). https://doi.org/10.1016/S0169-4332(03)00267-8.
18. S. Zeyrek, Ş Altındal, H. Yüzer, and M.M. Bülbül, Current transport mechanism in Al/Si3N4/p-Si (MIS) Schottky barrier diodes at low temperatures. *Appl. Surf. Sci.* 252, 2999 (2006). https://doi.org/10.1016/j.apsusc.2005.05.008.
19. Ö.F. Yüksel, Temperature dependence of current–voltage characteristics of Al/p-Si (100) Schottky barrier diodes. *Physica B* 404, 1993 (2009). https://doi.org/10.1016/j.physb.2009.03.026.
20. M.E. Aydın, Ö. Gülü, and N. Yıldırım, Temperature dependence of current–voltage characteristics of Sn/p-Si Schottky contacts. *Physica B* 403, 131 (2008). https://doi.org/10.1016/j.physb.2007.08.089.
21. M.O. Aboelfotoh, Electrical characteristics of Ti/Si (100) interfaces. *J. Appl. Phys.* 64, 4046 (1988).
22. U.H. Asıl, Comparison of I–V methods for determination of Ti/p-Si Schottky diode parameters. *Yüzüncü Yıl Univ. J. Inst. Nat. Appl. Sci.* 27, 158 (2022). https://doi.org/10.53433/yyufbed.1058643.
23. R. Kumar and S. Chand, Fabrication and electrical characterization of nickel/p-Si Schottky diode at low temperature. *Solid State Sci.* 58, 115 (2016). https://doi.org/10.1016/j.solidstatesciences.2016.06.003.
24. A. Kumar, A. Kumar, K.K. Sharma, and S. Chand, Analysis of anomalous transport mechanism across the interface of Ag/p-Si Schottky diode in wide temperature range. *Superlattices Microstruct.* 128, 373 (2019). https://doi.org/10.1016/j.spmi.2019.02.014.
25. S. Acar, S. Karadeniz, N. Tuğluoğlu, A.B. Selçuk, and M. Kasap, Gaussian distribution of inhomogeneous barrier height in Ag/p-Si (1 0 0) Schottky barrier diodes. *Appl. Surf. Sci.* 233, 373 (2004). https://doi.org/10.1016/j.apsusc.2004.04.011.
26. U.H. Asıl, D.K. Çınar, and C. Coşkun, The effect of thermal annealing on Ti/p-Si Schottky diodes. *J. Mater. Sci. Mater. Electron.* 32, 15343 (2021).
27. Ö.F. Bakkaloğlu, K. Ejderha, H. Efeoğlu, Ş Karataş, and A. Türüt, Temperature dependence of electrical parameters of the Cu/n-Si metal semiconductor Schottky structures. *J. Mol. Struct.* 1224, 129057 (2021). https://doi.org/10.1016/j.molstruc.2020.129057.
28. D.S. Reddy, M.B. Reddy, N.N. Kumar Reddy, and V. Rajagopal Reddy, Schottky barrier parameters of Pd/Ti contacts on N-type InP revealed from I–V–T And C–V–T measurements. *J. Mod. Phys.* 2, 113 (2011). https://doi.org/10.4236/jmp.2011.23018.
29. Y.P. Song, R.L. Van Meirhaeghe, W.H. Laflere, and E. Cardon, On the difference in apparent barrier height as obtained from capacitance–voltage and current–voltage–temperature measurements on Al/P-Inp Schottky barriers. *Solid-State Electron.* 29, 633638 (1986).
30. J. Chen, Q. Wang, J. Lv, H. Tang, and X. Li, Current–voltage–temperature and capacitance–voltage–temperature characteristics of TiW alloy/p-InP Schottky barrier diode. *J. Alloys Compd.* 649, 1220 (2015). https://doi.org/10.1016/j.jallcom.2015.07.239.
31. N.S. Shankar and R.V. Rajagopal, Analysis of current–voltage–temperature (I–V–T) and capacitance–voltage–temperature (C–V–T) characteristics of Ni/Au Schottky contacts on n-type InP. *Superlattices Microstruct.* 48, 330 (2010). https://doi.org/10.1016/j.spmi.2010.06.019.
32. S. Boughdachi, Y. Badali, Y. Azizian-Kalandaragh, and Ş Altındal, Current-transport mechanisms of the Al/(Bi2S3-PVA nanocomposite)/p-Si Schottky diodes in the temperature range between 220 K and 380 K. *J. Electron. Mater.* 47, 6945 (2018). https://doi.org/10.1007/s11664-018-6593-y.

33. R.F. Schmitsdorf, T.U. Kampen, and W. Mönch, Correlation between barrier height and interface structure of Ag/Si(111) Schottky diodes. *Surf. Sci.* 324, 249 (1995).
34. H. Altuntaş, A. Bengi, U. Aydemir, T. Asar, S.S. Çetin, I. Kars, S. Altındal, and S. Özçelik, Electrical characterization of current conduction in Au/TiO_2/n-Si at wide temperature range. *Mater. Sci. Semicond. Process.* 12, 224 (2009). https://doi.org/10.1016/j.mssp.2009.12.001.
35. B. Asha, C.S. Harsha, R. Padma, and V. Rajagopal-Reddy, Analysis of Schottky barrier parameters and current transport properties of V/p-type GaN Schottky junction at low temperatures. *J. Electron. Mater.* 47, 4140 (2018). https://doi.org/10.1007/s11664-018-6313-7.
36. E. Ayyıldız, H. Çetin, and Z. Horvath, Temperature dependent electrical characteristics of Sn/p-Si Schottky diodes. *J. Appl. Surf. Sci.* 252, 1153 (2005). https://doi.org/10.1016/j.apsusc.2005.02.044.

Publisher's Note Springer Nature remains neutral with regard to jurisdictional claims in published maps and institutional affiliations.